Agronomie 22 (2002) 627–633
© INRA, EDP Sciences, 2002
DOI: 10.1051/agro:2002032

Original article

Spatialization of sensible heat flux over a heterogeneous landscape

Jean-Pierre LAGOUARDE[a]*, Frédéric JACOB[b], Xing Fa GU[b], Albert OLIOSO[b], Jean-Marc BONNEFOND[a], Yann KERR[c], K. John MCANENEY[d], Mark IRVINE[a]

[a] INRA Bioclimatologie, BP 81, 33883 Villenave d'Ornon, France
[b] INRA Unité CSE, Domaine St-Paul, Site Agroparc, 84914 Avignon Cedex 9, France
[c] CESBIO, 18 avenue E. Belin, 31401 Toulouse, France
[d] Macquarie University, Sydney, NSW, Australia

(Received 2 October 2001; revised 10 December 2001; accepted 19 February 2002)

Abstract – Two methods for retrieving sensible heat flux over a bare soil/wheat composite surface are compared. The first one is based on field measurements using large aperture scintillometers. The comparison with reference fluxes obtained from eddy correlation technique shows that scintillometry-derived fluxes are overestimated by 10%. A numerical experiment demonstrates this is induced by the non-uniform sensitivity of the scintillometer to C_N^2 along the path length which follows a 'bell-shaped' curve. The second method is based on the use of a simple surface energy balance model, SEBAL, supplied with high spatial resolution remote sensing data from two airborne sensors in visible, near infrared and TIR bands. A comparison with scintillometry-derived fluxes shows important discrepancies. These result from large errors in the estimation of the roughness length z_0 in the model. This demonstrates that the use of an empirical relationship based on NDVI only is inadequate for inferring this key parameter in SEBAL.

sensible heat flux / structure parameter / optical scintillations / large aperture scintillometer / spatialized energy balance model

Résumé – Intégration spatiale du flux de chaleur sensible au-dessus d'un paysage hétérogène. Deux méthodes d'estimation du flux de chaleur sensible sur une surface composite sol nu/blé sont comparées. La première repose sur des mesures de terrain au moyen de scintillomètres à grande ouverture. La comparaison avec des mesures de référence effectuées par la technique des corrélations révèle une surestimation de 10 % sur les flux obtenus par scintillométrie. Des simulations numériques montrent que cela provient du fait que la sensibilité du scintillomètre au paramètre de structure le long du trajet optique n'est pas uniforme et suit une courbe en cloche. La seconde méthode est basée sur l'utilisation du modèle de surface SEBAL alimenté par des données de télédétection aéroportée dans les domaines visible, proche infrarouge et infrarouge thermique. On observe des différence très importantes avec la scintillométrie. Elles sont attribuées aux erreurs d'estimation de la rugosité dans le modèle, et montrent que l'utilisation d'une relation empirique basée sur le seul NDVI pour estimer ce paramètre-clé est insuffisante.

flux de chaleur sensible / paramètre de structure / scintillations optiques / scintillomètre à grande ouverture / spatialisation du bilan d'énergie

1. INTRODUCTION

The goal of estimating and mapping surface fluxes requires simultaneous research in several domains: development of models, integration of remote sensing data, and validation of the proposed methods by field measurements. These methods must be adapted to the European landscape, often characterized by a patchwork of small sized fields, and must be at the same time simple and reliable enough for practical applications. The Alpilles/ReSeDA joint experiment which took place in 1997 in the South-East of France [19] provided a good opportunity to test such approaches. With this idea we evaluated the SEBAL algorithm used in combination with high spatial resolution imagery in Visible-Near Infrared (Vis-NIR) and Thermal Infrared (TIR) domains. Obtaining fluxes directly measured at the intermediate kilometric scale for validation purposes still remains difficult: the technique of scintillometry could cover the gap presently existing between the field local scale measurements (typically the hundreds of meters with micrometeorological

Communicated by Frédéric Baret (Avignon, France)

* Correspondence and reprints
lagouarde@bordeaux.inra.fr

or eddy correlation stations) and the regional scale (i.e. ten kilometers at least with airborne atmospheric measurements). Scintillometry which has already been shown to provide good results for homogeneous surfaces was tested for the case of a two-field composite landscape in the Alpilles site and compared with the SEBAL model results.

2. EXPERIMENTAL

The experiment was performed in June 1997 over a composite surface bare soil (216 m)/wheat (451 m) at La Paillade (43°47'N, 4°45'E) composed of 3 fields (fields 120 and 124, 358 and 93 m long respectively, for wheat, and field 121, 216 m long, sown with sunflower but with bare soil conditions at the time of the experiment).

Two 'large aperture' scintillometers (LAS) were placed at 2.05 and 4.54 m heights between days 155 and 163. These instruments were provided by the Horticultural Research Institute (New Zealand) and are described in detail in [17]. Fields 120 and 121 were equipped with 3D sonic anemometers (Gill R3) and additional micrometeorological measurements were performed (air temperature and wind speed at the height of the scintillometers, net radiation, ground heat flux at 5 mm depth). A 1D Campbell sonic anemometer was installed in field 124. The fluxes derived from the scintillometers were compared with those estimated from eddy correlation measurements weighted by the dimension of the corresponding fields. A map of the site and a scheme of the experimental setup are given in Figures 1 and 2, respectively.

Airborne data were acquired using the imaging radiometer PolDER [8] and a thermal infrared camera INFRAMETRICS 760[1], both flown aboard an aircraft on June 9th (DoY 160). Five flight lines were completed between 11:50 and 12:25 UTC: four of them in the principal plane, and one in the perpendicular plane. The flight altitude was about 3000 m, yielding a 20 m nadir spatial resolution for both instruments.

[1] The names of companies are given for the benefit of the reader and do not imply any endorsement of the product or company by the authors.

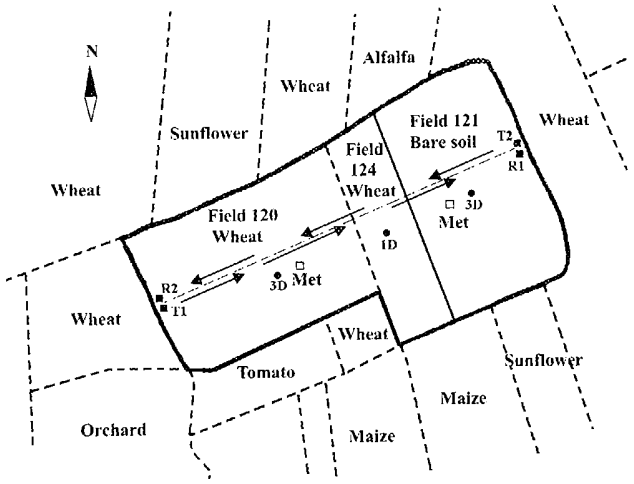

Figure 1. Map of the experimental site (details about the experimental setup given in next figure).

The PolDER measurements were multidirectional (± 50°) and performed in 40 nm width spectral bands centered on 443, 550, 670 and 865 nm. Data was processed in a similar way to that in [15] to derive samplings of the Bi-directional Reflectance Distribution Function (BRDF). The TIR INFRAMETRICS 760 data was acquired over the 7.25–13.25 μm spectral band. After radiometric corrections and image registrations [11], a multidirectional surface brightness temperature data set was finally provided.

3. ESTIMATION OF THE AREALLY-AVERAGED SENSIBLE HEAT FLUX BY SCINTILLOMETRY

3.1. Principle

Scintillometers provide a measurement of the structure parameter for the refractive index C_N^2 derived from the analysis of the intensity fluctuations of an optical beam between a

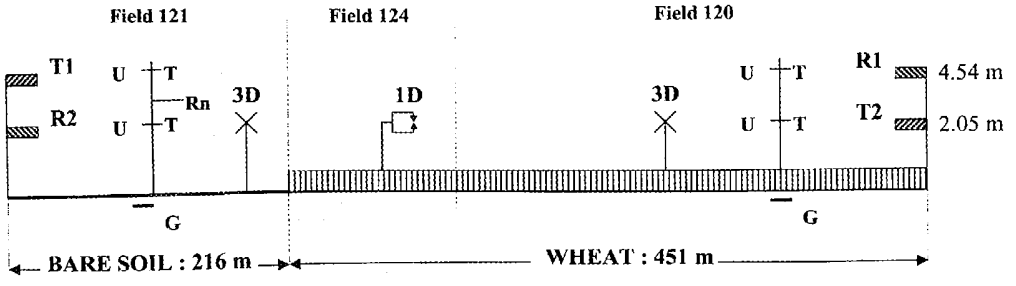

Figure 2. Experimental setup. (T1, R1) and (T2, R2) correspond to transmitters and receivers of scintillometers 1 and 2. 1D and 3D indicate sonic anemometers. Micrometeorological measurements (soil heat plates G, air temperature T, wind speed U, net radiation Rn) are also indicated.

transmitter and a receiver. A review can be found in [9]. We only give here a rapid overview of the method already described in detail by several authors in the case of uniform surfaces [7, 17]. In the optical domain, in which humidity fluctuations in the atmosphere have a much smaller influence than temperature fluctuations, the structure parameter for temperature C_T^2 can be derived from C_N^2 measured by a scintillometer by:

$$C_T^2 = C_N^2 \left(\frac{T_a^2}{\gamma P} \right) (1 + 0.03/\beta)^{-2} \quad (1)$$

P is the atmospheric pressure (Pa), T_a the air temperature (K), and γ a refractive index coefficient for air ($\gamma = 7.9 \times 10^{-7}$ K·Pa^{-1}). C_N^2 and C_T^2 are in $m^{-2/3}$ and $K^2 m^{-2/3}$ respectively. β is the Bowen ratio $\beta = H/(Rn-G-H)$, Rn and G being the net radiation and ground heat flux respectively. The temperature scale T_* (K) is retrieved from C_T^2:

$$C_T^2 = T_*^2 z^{-2/3} f(z/L) \quad (2)$$

where z is the height corrected from the displacement height d. We used the classical expressions of the f function proposed by Wyngaard [23]:

$$f(z/L) = 4.9\left(1 + 7\left|\frac{z}{L}\right|\right)^{-2/3} \quad \text{for } z/L < 0 \text{ (unstable)} \quad (3)$$

$$f(z/L) = 4.9\left(1 + 2.4\left|\frac{z}{L}\right|\right)^{-2/3} \quad \text{for } z/L > 0 \text{ (stable)} \quad (4)$$

L is the Monin-Obhukov length defined as:

$$L = -\frac{T_a u_*^2}{k\, g\, T_*} \quad \text{with } k = 0.4 \text{ and } g = 9.81 \text{ m·s}^{-2}. \quad (5)$$

A wind speed measurement allows the determination of the friction velocity u_*, assuming the roughness length z_0 to be known, as:

$$u_* = k\, u \left[\ln\left(\frac{z}{z_0}\right) - \psi_M\left(\frac{z}{L}\right) \right]^{-1} \quad (6)$$

where Ψ_M is the classical stability function given by Panofsky and Dutton [18].

The sensible heat flux H (W·m^{-2}) is then computed as:

$$H = \rho\, c_p\, u_*\, T_* \quad (7)$$

ρ (kg·m^{-3}) and c_p (J·kg^{-1}·K^{-1}) are the air density and heat capacity, respectively. u_* is in m·s^{-1}. Since the sensible heat flux determines atmospheric stability, which in turn influences turbulent transport, an iterative procedure is necessary.

This method has been successfully tested in the case of homogeneous surfaces: pasture [17] and vineyards [7] among others. Its application to the case of composite landscape presents several theoretical problems:

- The assumption the Monin-Obhukov similarity theory (MOST) still holds is questionable: the physical meaning of the 'equivalent' or 'averaged' temperature scale T_* – as globally retrieved from a single scintillometer measurement over a composite path length – remains unclear, as well as the meaning of the friction velocity u_*.
- This fundamental question apart, we are faced with several problems of parameterization which are presented below.
- Finally, despite a significant amount of work during the past few years [3, 6, 10], local advection which affects the transition between fields and largely depends on the combination of several factors (surface characteristics upwind and downwind, wind direction...) still remains difficult to take into account.

3.2. Application to a composite surface

The sensitivity of the scintillometer to C_N^2 along the beam is not uniform and follows a bell-shape curve [21]. For equal transmitter and receiver apertures, this curve is symmetrical (Fig. 3). If W(y) is the weighing function (with y normalized distance, i.e. $y = x/L_{beam}$, L_{beam} being the path length and x the distance from one of its extremities) and $C_N^2(y)$ the value of the structure parameter at distance y, the average structure parameter on the optical path $\langle C_N^2 \rangle$ is given by [21]:

$$\langle C_N^2 \rangle = \int_0^1 C_N^2(y)\, W(y)\, dy. \quad (8)$$

For a two component surface which is the case studied in this paper, equation (8) can be written:

$$\langle C_N^2 \rangle = C_{N1}^2\, W_1 + C_{N2}^2\, W_2 \quad (9)$$

$$\text{with } W_1 = \int_0^r W(y)dy \text{ and } W_2 = \int_r^1 W(y)dy \quad (10)$$

r is the ratio of the length of surface 1 to the total path length. C_{N1}^2 and C_{N2}^2 are the structure parameters for refractive index for surfaces 1 and 2. We obviously have $W_1 + W_2 = 1$. Lagouarde et al. [13] experimentally verified equation (9).

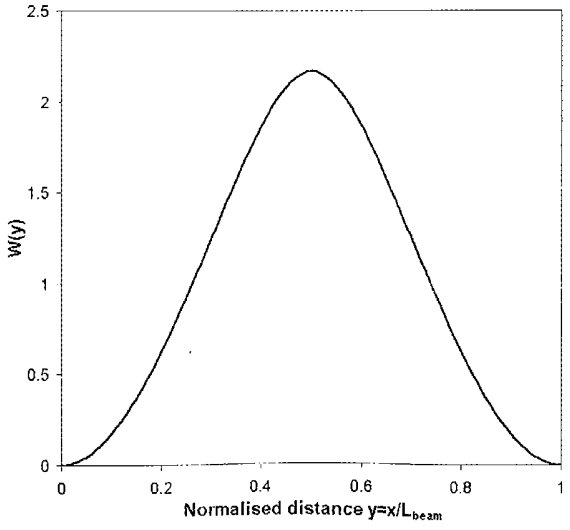

Figure 3. Weighing function of the scintillometer. y is the path distance x from the transmitter normalized by the total length of the path L_{beam}.

Practical application of the above-described method to composite surfaces requires defining several aggregation schemes to estimate equivalent quantities indicated by symbols < > in what follows.

The two measurements of wind speed at the same height over the two surfaces were averaged according to a scheme based on the statement that the transit time of a particle of air transported along the path length is the sum of the transit times over each surface. It leads to:

$$< u > = \frac{u_1 \, u_2}{r\,u_2 + (1-r)u_1} \qquad (11)$$

where u_1 and u_2 are the wind speed measurements over surfaces 1 and 2.

As it always appears through the term z-d, the sensitivity to the displacement height is limited. We therefore only considered one simple aggregation scheme consisting of a linear averaging of the displacement heights d_1 and d_2 over each surface:

$$< d > = r\,d_1 + (1-r)\,d_2 \qquad (12)$$

Two aggregation schemes have been tested for roughness length which is an important key parameter. For the two surface composite case, the first one [20], referred to as RL1, can be written:

$$\mathrm{Ln} < z_0 > = r\,\mathrm{Ln}(z_{01}) + (1-r)\,\mathrm{Ln}(z_{02}) \qquad (13)$$

According to Mason [16] and Claussen [5] we also examined (scheme RL2):

$$\frac{1}{\left[\mathrm{Ln}\left(\frac{z - < d >}{< z_0 >}\right)\right]^2} = \frac{r}{\left[\mathrm{Ln}\left(\frac{z-d_1}{z_{01}}\right)\right]^2} + \frac{1-r}{\left[\mathrm{Ln}\left(\frac{z-d_2}{z_{02}}\right)\right]^2} \qquad (14)$$

3.3. Results

The roughness lengths of wheat and bare soil were first estimated from wind speed (u), friction velocity (u_*) and Monin-Obukhov length (L) values obtained from the 3D sonic anemometer measurements. We used equation (6) inverted and we only considered near-neutral conditions for which $-0.2 \leq z/L \leq 0$. We took displacement heights d = 0 for bare soil and d = 0.5 m for wheat. For wheat it was assessed from the canopy height h_c as $d \sim 0.66\ h_c$ [4]. The derived roughness length values were $z_0 \sim 0.007$ m for bare soil and $z_0 \sim 0.10$ m for wheat with standard deviations 0.004 m and 0.03 m respectively. These are consistent with general experience, and the value found for wheat perfectly fits the classical rule of thumb $z_0 \sim 0.13\ h_c$ for dense vegetation canopies.

Figure 4 displays the comparison between sensible heat flux obtained by scintillometry with reference values H_{ref}. The sensible heat flux was calculated at both levels 2.05 and 4.54 m. The scintillometer measurements were combined with the meteorological data (wind speed and air temperature) acquired at the same heights. H_{ref} is the average of the measurements (by eddy correlation technique) of sensible heat flux weighed by the ratio of the corresponding fields: $H_{ref} = 0.537\ H_{120} + 0.139\ H_{124} + 0.324\ H_{121}$. The comparison

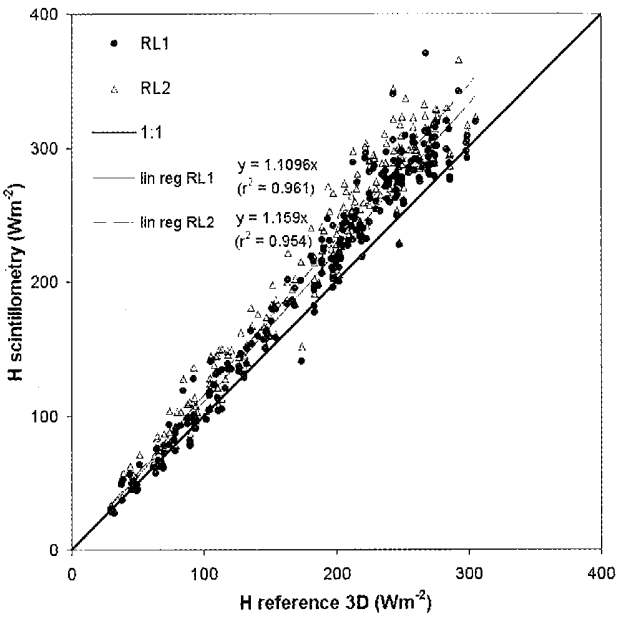

Figure 4. Comparison between spatially-averaged sensible heat flux derived from eddy correlation measurements and from scintillometry, using 2 aggregation schemes for roughness length. Regression lines are also plotted.

of the two wheat fields revealed that field 124 was a little drier than 120: we found a regression $H_{124(1D)} = 1.153\ H_{120(3D)}$ ($r^2 = 0.893$, rmse = 34.0 W·m^{-2}). This relation was used to extrapolate some missing data in field 124.

Figure 4 reveals a systematic bias with an overestimation of the scintillometer-derived flux by about 11% and 16% for aggregation schemes RL1 and RL2 respectively. We did not notice significant sensitivity to measurement height or to wind direction. After careful investigations not described in detail here (intercalibration of instruments, and analysis of the possible contribution of low frequencies in the 3D sonic anemometers' measurements particularly...) we could not find any obvious experimental reason to explain either overestimation of H by scintillometers or underestimation by sonic anemometers. The bias observed in Figure 4 is therefore likely not to be an artefact, and we suspected that the aggregation process of the C_N^2 along the beam could be responsible for it. As a matter of fact, it includes several sources of non-linearity: non-linearity of the relationship between H and C_N^2, and non-linearity of the scintillometer sensitivity along the beam.

3.4. Simulation

We assumed a composite area including 2 surfaces. The principle of the simulation consisted of 3 steps:

(i) estimating the structure parameters C_{N1}^2 and C_{N2}^2 for both surfaces from prescribed values of fluxes H_1 and H_2 by

using the method described in Section 3.1. in backward mode. Also prescribed the surface parameters (roughness length and displacement height were given different values for both plots) and the micrometeorological variables (air temperature and wind speed at 10 m, both assumed uniform over the composite area). The computations successively consisted of retrieving u_* from equation (6) (an iterative procedure is here necessary as u_* appears of the expression of L), deriving T_* from equation (7), and finally estimating C_T^2 and C_N^2 from equations (1) and (2);

(ii) weighing C_{N1}^2 and C_{N2}^2 according to the bell-shaped sensitivity curve of the scintillometer (Eq. (9)) to simulate the scintillometer-measured C_N^2;

(iii) computing the areally-averaged sensible heat flux H_{sim} following Section 3.1. (forward mode). This was finally compared to the reference prescribed H_{presc} value consisting of the linear weighing of the initially prescribed fluxes $H_{presc} = r H_1 + (1 - r) H_2$. (15)

Figure 5 displays the results obtained when giving both surfaces the actual values of parameters z_0 and d, and the variables (H_1, H_2, micrometeorological data) measured at every time step during the experiment. The bias we already noted is still visible. As can be seen in Table I, which gives the slopes of the different regression lines (forced through the origin), it is about 5% lower than the one found in the field experiment. Nevertheless, as the simulation procedure obviously eliminates the influence of any possible instrumental error, it confirms that an important part of the bias is inherent in the scintillometry technique when applied to composite areas. It

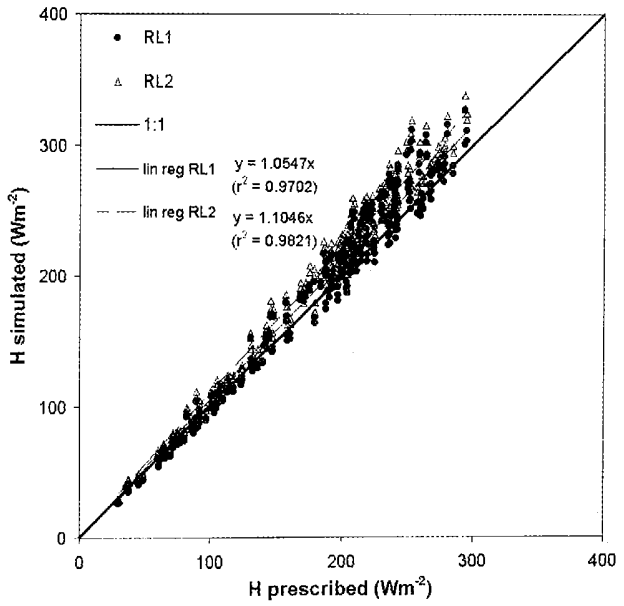

Figure 5. Simulation of the scintillometer response for a two-surface composite path length: comparison between simulated and prescribed areally-averaged sensible heat flux. Regression lines are indicated.

Table I. Slope of the regression lines obtained when comparing H estimates for experimental data (comparison between scintillometry and eddy correlation measured H) and for simulation (comparison between simulated and prescribed H, see text).

	RL1	RL2
Field data	1.110	1.159
Simulation	1.055	1.105

results from the non-uniform sensitivity of the instrument to C_N^2 along the path length and depends on the characteristics of the composite area: the ratio of both plots, difference in their aerodynamic characteristics (mainly roughness) and contrast in their surface fluxes. A systematic study based on numerical experiments to assess the influence of each of these factors can be found in [14]. Advection effects could also be invoked to explain another part of the bias. De Bruin et al. [6] found too large on air temperature variance under local advective conditions As a consequence, it can be expected that scintillometers tend to overestimate fluxes in such conditions.

4. ESTIMATION OF THE SENSIBLE HEAT FLUX USING THE SEBAL MODEL

4.1. Description of the model

The single layer SEBAL model (Surface Energy Balance Algorithm for Land [1, 2] aims at mapping surface energy fluxes using exclusively multispectral remote sensing data. Its interest is to estimate both wind speed and air temperature from the information contained in the spatial variability of surface albedo and temperature. This assumes that the study area includes sites with very high and very low evapotranspiration. The model requires maps of NDVI (Normalized Difference Vegetation Index), albedo and surface brightness temperature. It computes the surface energy fluxes at the same spatial resolution as input maps. A more detailed description of SEBAL can be found in [11]. Note only here that the roughness length z_0 is estimated from NDVI through a semi-empirical relationship. In the original version of the model [1], we find:

$$z_0 = \exp(6.38\ \mathrm{NDVI} - 6.665). \quad (16)$$

4.2. SEBAL results

The multidirectional POLDER data were used with linear kernel-driven BRDF models to compute both the nadir and hemispherical reflectances. NDVI was calculated as the normalized difference between the 865 and 670 nm nadir reflectances. Albedo was computed as a linear combination of the hemispherical reflectances in the four POLDER channels [12, 22]. To provide the surface brightness temperature maps, we averaged the INFRAMETRICS 760 data corresponding to nadir view angles lower than 20°. SEBAL maps

of sensible heat fluxes showed a significant spatial variability for heterogeneous fields, and the pattern of the whole site at a larger scale. The reader will find a more detailed description of the methods used to derive the SEBAL input variables in [11], as well as a comparison of model outputs with field measurements.

We then computed averaged values of the SEBAL-derived sensible heat fluxes over the fields 120, 121, 124 (after elimination of the edges possibly contaminated by adjacent fields) and along the scintillometer optical path (Fig. 6). The ratio of the averaged values between fields 124 and 120 was about 1.14, which was close to eddy correlation measurements (Sect. 3.3.). Table II displays the comparison between SEBAL and ground measurements for fields 120 and 121 independently, and then integrated along the scintillometer optical path. A first simulation performed with the initial version of the SEBAL model led to a very large underestimation of H_{path}. This was clearly related to erroneous estimation of H_{120} over wheat. As the model estimates of the net radiation and of the difference between surface and air temperatures were correct, the origin of the discrepancy on H_{120} could only be found in the unrealistic estimate of z_0 provided by SEBAL: 0.01 m compared with the 0.1 m reference value derived from 3D eddy correlation measurements. The reason is obviously the failure of the semi-empirical relationship between z_0 and NDVI in our case: at the beginning of the senescence phase, the drying wheat keeps its structure (height, leaves...) and hence its roughness, but displays a dramatic decrease in NDVI. This was confirmed by a second simulation in which the roughness lengths for wheat and bare soil were prescribed to the reference values, 0.1 and 0.007 m, respectively: the agreement obtained on H_{path} is much better (see Tab. II).

Table II. Comparison between reference eddy correlation-derived, scintillometry-derived, and SEBAL-derived estimates of sensible heat flux for fields 120 and 121 and integrated over the scintillometer path length.

	H_{120} Wheat	H_{121} Bare soil	H_{path} Optical path
Eddy correlation	303.1	188.6	273.0
Scintillometer	–	–	296.9
SEBAL (initial version)	122.1	174.5	141.4
SEBAL (z_0 prescribed)	242.8	205.6	240.9

5. CONCLUSION

In this paper two methods for inferring spatially-averaged sensible heat flux have been tested. For the simple case of a two-surface composite landscape, scintillometry provided slightly overestimated values compared to reference eddy correlation measurements by about 10%. A simple model of the scintillometer response confirmed that the deviation results from non-linearities in the integration process of the scintillometer signal along the optical path. In the framework of another paper [14], this model has been used to study the sensitivity of scintillometer measurements to the characteristics of the surface (composition, contrasts in fluxes and roughness between plots) and to derive a method for correcting the bias in H. The very large discrepancies observed between reference H values (from eddy correlation) and the SEBAL model-derived ones were attributed to errors in the estimates of roughness length rising from the inadequacy of the semi-empirical relationship between NDVI and z_0 used. This example once more illustrates the well-known difficulty of finding a satisfactory compromise between the simplifications of models, brought about by the use of very coarse parameterizations, and their accuracy.

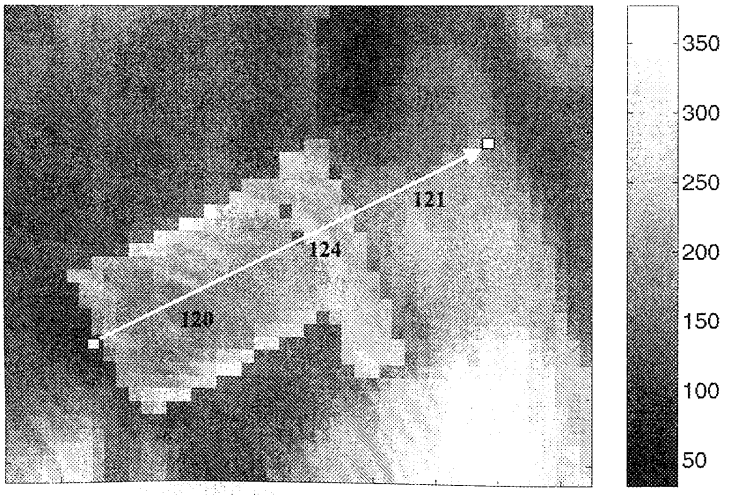

Figure 6. SEBAL-derived sensible heat flux (in $W \cdot m^{-2}$) for fields 120, 121 and 124. The white line corresponds to the scintillometer optical path.

Acknowledgments: The Alpilles-ReSeDA project was funded by the EEC-DG XII and by the French Programme National de Télédétection Spatiale and Programme National de Recherches en Hydrologie. Financial support for this study was also provided by the EC in the framework of the WATERMED project (contract ICA3-CT-1999-00015). The IRSA-MARS project provided access to ground data and SPOT images. The PoLDER airborne sensor was provided by the LOA (Lille, France). The authors also thank the Horticultural Research Institute (New Zealand) who provided the scintillometers and experimental support. Part of this study was founded by EC in the frame of the WATERMED project (Contact ICA3-CT-1999-00015).

REFERENCES

[1] Bastiaanssen W.G.M., Menenti M., Feddes R.A., Holtslag A.A.M., A remote sensing surface energy balance algorithm for land (SEBAL). 1. Formulation, J. Hydrol. 212–213 (1998) 198–212.

[2] Bastiaanssen W.G.M., Pelgrum H., Wang J., Ma Y., Moreno J., Roerink G., Van der Wal T., A remote sensing surface energy balance algorithm for land (SEBAL). 2. Validation, J. Hydrol. 212–213 (1998) 213–292.

[3] Brunet Y., Itier B., McAneney K.J., Lagouarde J.P., Downwind evolution of scalar fluxes and surface resistance under conditions of local advection. Part II: measurements over barley, Agric. For. Meteorol. 71 (1994) 227–245.

[4] Brutsaert W., Evaporation into the atmosphere. Theory, History and Applications, D. Reidel publishing Company, Dordrecht, Holland, 1982, 299 p.

[5] Claussen M., Estimation of areally-averaged surface fluxes, Bound.-Layer Meteorol. 54 (1991) 387–410.

[6] De Bruin H.A.R., Bink N.J., Kroon L.J.M., Fluxes in the surface layer under advective conditions, in: Schmugge T.J., André J.C. (Eds.), Land Surface Evaporation, Measurement and Parameterization, Berlin, Springer Verlag, pp. 157–171.

[7] De Bruin H.A.R., Van den Hurk B.J.J.M., Kohsiek W., The scintillation method tested over a dry vineyard area, Bound.-Layer Meteorol. 76 (1995) 25–40.

[8] Deschamps P.Y., Bréon F.M., Leroy M., Podaire A., Bricaud A., Buriez J.C., Sèze G., The POLDER mission: instrument characteristics and scientific objective, IEEE Trans. Geosci. Remote Sens. 32 (1994) 598–615.

[9] Hill R.J., Review of optical scintillation methods of measuring the refractive-index spectrum, inner scale and surface fluxes, Waves in Random Media 2 (1992) 179–201.

[10] Itier B., Brunet Y., McAneney K.J., Lagouarde J.-P., Downwind evolution of scalar fluxes and surface resistance under conditions of local advection. Part I: a reappraisal of boundary conditions, Agric. For. Meteorol. 71 (1994) 211–225.

[11] Jacob F., Utilisation de la télédétection courtes longueurs d'onde et infrarouge thermique à haute résolution spatiale pour l'estimation des flux d'énergie à l'échelle de la parcelle agricole, Thèse de Doctorat, 1999, Université de Toulouse III (Spécialité : Télédétection de la Biosphère Continentale), 268 p.

[12] Jacob F., Olioso A., Weiss M., Baret F., Hautecœur O., Hanocq J.-F., Mapping short-wave albedo of agricultural surfaces using airborne POLDER data, Remote Sens. Environ. 80 (2002) 36–46.

[13] Lagouarde J.-P., McAneney K.J., Green A.E., Spatially-averaged measurements of sensible heat flux using scintillations: first results above a heterogeneous surface, "Scaling-up in Hydrology using remote sensing" workshop, June 10-12 1996, Institute of Hydrology, Wallingford G.B., Wiley & Sons Ed. (1996), pp. 147–160.

[14] Lagouarde J.-P., Bonnefond J.-M., Kerr Y.H., McAneney K.J., Irvine M., Integrated sensible heat flux measurements of a two-surface composite landscape using scintillometry, Bound.-Layer Meteorol. (2002) special issue, in press.

[15] Leroy M., Hautecœur O., Directional parameters, hemispherical reflectances and angle-corrected NDVIs derived at global scale by the spaceborne POLDER, Proc. Alps99 conférence, Méribel France, January 18-22, CNES Ed. (1999), 'Land surfaces' Session, pp. 1–4.

[16] Mason P.J., The formation of areally-averaged roughness lengths, Quart. J. Roy. Meteorol. Soc. 114 (1988) 399–420.

[17] McAneney K.J., Green A.E., Astill M.S., Large-aperture scintillometry: the homogeneous case, Agric. For. Meteorol. 76 (1995) 149–162.

[18] Panofsky H.A., Dutton J.A., Atmospheric turbulence: models and methods for engineering applications, John Wiley & Sons (1984), New York, 397 p.

[19] Prévot L., et al., Assimilation of multi-sensor and multi-temporal remote sensing data to monitor vegetation and soil: the Alpilles-ReSeDA project. IGARSS'98, Int. Geosci. Remote Sens. Symp., Ed. L. Tsang, Seattle (1998), pp. 17–30.

[20] Taylor P.A., Comments and further analysis on effective roughness lengths for use in numerical three-dimensional models, Bound.-Layer Meteorol. 39 (1987) 403–418.

[21] Wang Ting-i, Ochs G.R., Clifford S.F., A saturation-resistant optical scintillometer to measure C_N^2, J. Opt. Soc. Am. 68 (1978) 334–338.

[22] Weiss M., Baret F., Leroy M., Bégué A., Hautecœur O., Santer R., Hemispherical reflectance and albedo estimate from the accumulation of across-track sun-synchronous satellite data, J. Geophys. Res. 104 (1999) 2221–2232.

[23] Wyngaard J.C., On surface-layer turbulence. Workshop on Micrometeorology, Denver, Colorado, Am. Meteorol. Soc. (1973), pp. 101–149.